Catalysis Today 147S (2009) S113–S119

Contents lists available at ScienceDirect

Catalysis Today

journal homepage: www.elsevier.com/locate/cattod

The effective thermal conductivity of monolith honeycomb structures

R.E. Hayes *, A. Rojas, J. Mmbaga

Department of Chemical and Materials Engineering, University of Alberta, Edmonton, Alberta, Canada T6G 2G6

ARTICLE INFO

Article history:
Available online 29 July 2009

Keywords:
Monolith
Thermal conductivity
Washcoat

ABSTRACT

Recent advances in computational hardware and software have made it much easier to solve complex conduction problems numerically. In this work, a numerical investigation was performed to study the effective thermal conductivity as a function of monolith structure, washcoat presence and physical and geometrical properties. Both solid and fluid were spatially discretized and the resulting heat flux analyzed. The results are compared to those predicted using the electrical network analogy considering the monolith cell as a combination of series and parallel resistances. It is found that the analogy is not exact, and that a model based on a parallel resistance combination usually gave better results. The best value can be obtained by modelling the heat flow through a two dimensional web, which is not computationally expensive.

1. Introduction

The catalytic monolith reactor is widely used in catalytic combustion, with applications in the automotive industry (catalytic converters, diesel particulate filters) and others (gas turbines) [1]. It is also used or considered for other general chemical processing applications. The supporting substrate may be either metal or ceramic having a variety of cross-sectional shapes: square, hexagonal or triangular. There is an interest in using monolith of very high thermal conductivity in specialist applications, in which lower porosity monoliths are used with a substrate of high thermal conductivity. A monolith honeycomb is a structured porous medium.

Typically, a continuum model is used to model the monolith. One of the issues with continuum models is to use the correct values for the volume averaged or effective transport properties. In this paper, we restrict ourselves to the effective value of the thermal conductivity to be used in a monolith honeycomb matrix. The purpose of this paper is to examine and determine optimal models for effective thermal conductivity in the streamline direction (axial) and transverse to the flow (radial). The current proposed models in the literature are examined and compared to numerical solutions of the complete discrete problem.

2. Theoretical models for the effective thermal conductivity

An effective thermal conductivity for a composite system is often calculated using an overall resistance from network analysis. In this method the resistance of section is combined as a set of series and parallel resistances using network addition rules [2]. Although this method is not exact for resistances in parallel, it has been used for porous media, including heat transfer by conduction [3–5] and mass transfer by diffusion [6] in monolith systems.

Consider a three-dimensional monolith with flow in the z direction, and the x and y directions orthogonal to the direction of flow. The steady state fluid and solid equations for the heat transfer for the heterogeneous model can be respectively written as:

$$\frac{d}{dz}\left(k_{af,\mathrm{eff}}\frac{dT_f}{dz}\right) - v_s\rho_f C_{P,f}\frac{dT_f}{dz} + ha_v(T_S - T_f) = 0 \quad (1)$$

$$\frac{\partial}{\partial x}\left(k_{r,\mathrm{eff}}\frac{\partial T_s}{\partial x}\right) + \frac{\partial}{\partial y}\left(k_{r,\mathrm{eff}}\frac{\partial T_s}{\partial y}\right) + \frac{\partial}{\partial z}\left(k_{as,\mathrm{eff}}\frac{\partial T_s}{\partial z}\right) + ha_v(T_f - T_S) = 0 \quad (2)$$

For the fluid equation, the effect of thermal conductivity is sometimes eliminated, as it is often relatively small. All radial (transverse) conduction is assumed to occur in the solid phase equation. This approach is somewhat different from many heterogeneous models for unstructured porous media, where radial and axial conduction is included in both fluid and solid equations. In the homogeneous heat transfer model, a single energy balance is used, viz.:

$$\frac{\partial}{\partial x}\left(k_{r,\mathrm{eff}}\frac{\partial T}{\partial x}\right) + \frac{\partial}{\partial y}\left(k_{r,\mathrm{eff}}\frac{\partial T}{\partial y}\right) + \frac{\partial}{\partial z}\left(k_{as,\mathrm{eff}}\frac{\partial T}{\partial z}\right) - v_s\rho_f C_{P,f}\frac{\partial T}{\partial z} = 0 \quad (3)$$

* Corresponding author.
E-mail address: bob.hayes@ualberta.ca (R.E. Hayes).

0920-5861/$ – see front matter © 2009 Elsevier B.V. All rights reserved.
doi:10.1016/j.cattod.2009.07.005

Nomenclature

a_v	heat transfer area per unit volume (m^2/m^3)
b_S	inside dimension before washcoat applied (m)
b_W	inside dimension after washcoat applied (m)
$C_{P,f}$	heat capacity of the fluid (J/(kg K))
G	scaling factor for calculating effective conductivity
h	heat transfer coefficient (W/(m^2 K))
$k_{af,\text{eff}}$	effective axial thermal conductivity of fluid (W/(m K))
$k_{as,\text{eff}}$	effective axial thermal conductivity of solid (W/(m K))
$k_{as,eq}$	equivalent axial thermal conductivity of solid (W/(m K))
$k_{r,\text{eff}}$	effective radial thermal conductivity of solid (W/(m K))
k_W	thermal conductivity of the washcoat (W/(m K))
k_f	thermal conductivity of the fluid (W/(m K))
k_S	thermal conductivity of the substrate (W/(m K))
L	length in flow direction (m)
R	thermal resistance (K/W)
t_S	thickness of substrate (m)
T_f	temperature of the fluid (K)
T_S	temperature of the solid (K)
t_W	thickness of washcoat (m)
v_S	superficial fluid velocity (m/s)
W	overall cell dimension (m)
x	coordinate (m)
y	coordinate (m)
z	axial coordinate (m)

Greek letters

λ	volume fraction of substrate
ξ	volume fraction of washcoat
ϕ	volume fraction of voids (porosity after washcoat applied)
ρ_f	density of the fluid/kg/m^3

Note that the same value for the transverse thermal conductivity is typically used for both the heterogeneous and pseudo-homogeneous models, while for the axial conductivity they are different. The most commonly considered case, and the easiest for which to derive a theoretical model, is a monolith comprised of square cells with a uniformly distributed washcoat. The end view of a single cell for this case is shown in Fig. 1.

2.1. The effective axial conductivity

The main interest in this work is the radial conduction, however, for completeness we also describe the axial term. Consider first the heterogeneous reactor model. The axial conduction in the fluid phase occurs in the volume fraction occupied by the fluid, and therefore, for laminar flow, the effective axial thermal conductivity in the fluid phase in Eq. (1) is simply the thermal conductivity of the fluid multiplied by the porosity:

$$k_{a,\text{eff}} = \phi k_f \tag{4}$$

The axial thermal conductivity of the solid phase has a contribution from both the substrate and washcoat. When there is no washcoat, or when the thermal conductivity of the washcoat and the substrate are the same, the effective axial thermal conductivity in Eq. (2) is:

$$k_{as,\text{eff}} = (1-\phi)k_S = (\lambda+\xi)k_S \tag{5}$$

When the thermal conductivity of the substrate and washcoat are different, the resistance in parallel analogy can be used. The conduction resistance over an arbitrary length L for the substrate and washcoat can be expressed as:

$$R_S^{-1} = \left(\frac{\lambda W^2}{L}\right)k_S \quad \text{and} \quad R_W^{-1} = \left(\frac{\xi W^2}{L}\right)k_W \tag{6}$$

The equivalent resistance is written in terms of an equivalent conductivity and total solid area:

$$R_{eq}^{-1} = \left(\frac{(\lambda+\xi)W^2}{L}\right)k_{as,eq} \tag{7}$$

However, the effective thermal conductivity in the solid phase is based on the total area, thus:

$$R_{eq}^{-1} = \left(\frac{W^2}{L}\right)k_{as,\text{eff}} \tag{8}$$

Combining Eqs. (6) and (8) in the usual way gives:

$$R_{eq}^{-1} = R_S^{-1} + R_W^{-1} \tag{9}$$

or

$$\left(\frac{W^2}{L}\right)k_{as,\text{eff}} = \left(\frac{\lambda W^2}{L}\right)k_S + \left(\frac{\xi W^2}{L}\right)k_W \tag{10}$$

Eq. (10) simplifies to:

$$k_{as,\text{eff}} = k_S\left(\lambda + \frac{k_W}{k_S}\xi\right) \tag{11}$$

Eq. (11) has been reported in earlier work [3–5].

For the homogeneous model, the fluid and two solids comprise three resistances in series. The fluid resistance can be added to Eq. (10) to give:

$$\left(\frac{W^2}{L}\right)k_{as,\text{eff}} = \left(\frac{\phi W^2}{L}\right)k_f + \left(\frac{\lambda W^2}{L}\right)k_S + \left(\frac{\xi W^2}{L}\right)k_W \tag{12}$$

or

$$k_{as,\text{eff}} = \phi k_f + \lambda k_S + \xi k_W \tag{13}$$

For the special case where the washcoat is absent or has a thermal conductivity equal to the substrate, Eq. (13) simplifies to:

$$k_{as,\text{eff}} = \phi k_f + (1-\phi)k_S \tag{14}$$

Eq. (14) is widely used to model effective thermal conductivity in unstructured porous media. Although Eqs. (13) and (14) are illustrated for the case of a uniform washcoat and square channel, the results are the same for any channel geometry and washcoat distribution, provided that the cross-sectional area of each phase is constant over the axial distance.

2.2. The effective radial conductivity

Consider the effective radial (transverse) conductivity using the network analogy of series and parallel resistances with the geometry of Fig. 1. We develop the model in terms of the relative proportions of each constituent, which can be defined in terms

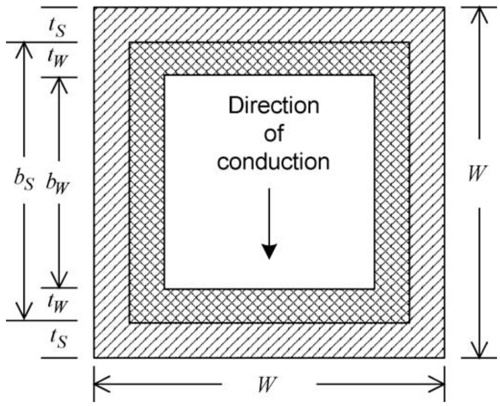

Fig. 1. End view of a single monolith cell with uniform washcoat.

of the geometry as:

$$\phi = \left(\frac{b_W}{W}\right)^2 \quad \lambda = \frac{W^2 - b_S^2}{W^2} \quad \xi = \frac{b_S^2 - b_W^2}{W^2} \tag{15}$$

The equivalent resistance can be defined with the two circuits shown in Fig. 2. For the circuit of Fig. 2(a), the equivalent resistance is:

$$R_{eq}^{-1} = 2R_1^{-1} + 2(2R_2 + R_3)^{-1} + (2R_4 + 2R_5 + R_6)^{-1} \tag{16}$$

The individual resistances are defined by:

$$R_1^{-1} = \frac{t_S}{W}k_S; \quad R_2^{-1} = \frac{t_W}{t_S}k_S; \quad R_3^{-1} = \frac{t_W}{b_S}k_W; \quad R_4^{-1} = \frac{b_W}{t_S}k_S; \quad R_5^{-1} = \frac{b_W}{t_W}k_W; \quad R_6^{-1} = k_f; \quad R_{eq}^{-1} = k_{r,\mathrm{eff}} \tag{17}$$

The resistances can also be defined in terms of the volume fractions occupied by each material, which is useful in generalizing the approach. Using Eq. (15) we can derive:

$$2\frac{t_S}{W} = 1 - \sqrt{\phi + \xi}; \quad \frac{b_S}{W} = \sqrt{\phi + \xi}; \quad \frac{b_W}{W} = \sqrt{\phi}; \quad 2\frac{t_W}{W} = \sqrt{\phi + \xi} - \sqrt{\phi} \tag{18}$$

Combining Eqs. (16)–(18) gives, after some manipulation, the final result:

$$k_{r,\mathrm{eff}} = \left[1 - \sqrt{\phi+\xi} + \frac{\sqrt{\phi+\xi} - \sqrt{\phi}}{1 - \sqrt{\phi+\xi} + (k_S/k_W)\sqrt{\phi+\xi}} + \frac{\sqrt{\phi}}{1 - \sqrt{\phi+\xi} + (k_S/k_W)(\sqrt{\phi+\xi} - \sqrt{\phi}) + (k_S/k_f)\sqrt{\phi}}\right] k_S \tag{19}$$

For the case without washcoat, the equation reduces to:

$$k_{r,\mathrm{eff}} = \left[1 - \sqrt{\phi} + \frac{\sqrt{\phi}}{1 - \sqrt{\phi} + (k_S/k_f)\sqrt{\phi}}\right] k_S \tag{20}$$

For reference purposes, we will refer to this model as the parallel model. Next consider the circuit of Fig. 2(b), where the maximum amount of series coupling is used. The equivalent

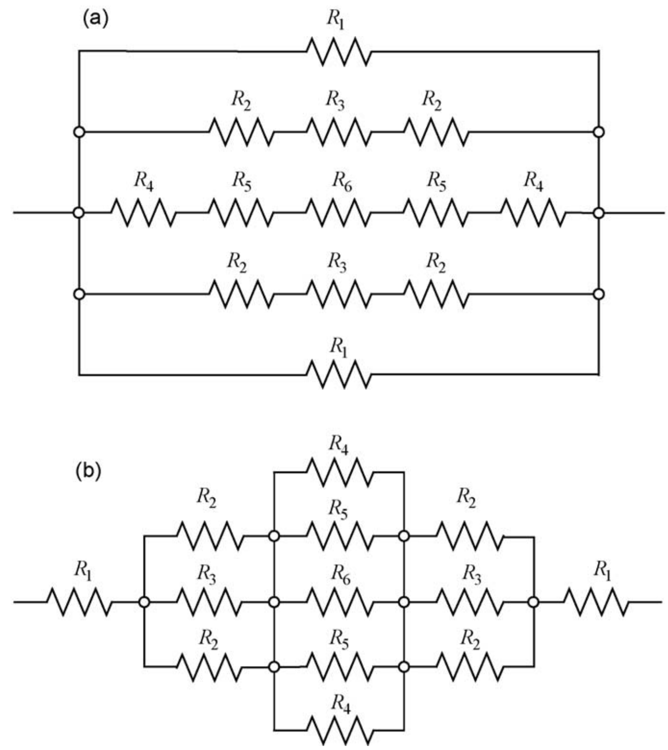

Fig. 2. Equivalent electrical circuit with (a) all systems in parallel and (b) series and parallel resistances.

resistance of the circuit is:

$$R_{eq} = 2R_1 + 2(2R_2^{-1} + R_3^{-1})^{-1} + (2R_4^{-1} + 2R_5^{-1} + R_6^{-1})^{-1} \tag{21}$$

The resistances are defined by:

$$R_1^{-1} = \frac{W}{t_S}k_S; \quad R_2^{-1} = \frac{t_S}{t_W}k_S; \quad R_3^{-1} = \frac{b_S}{t_W}k_W; \quad R_4^{-1} = \frac{t_S}{b_W}k_S; \quad R_5^{-1} = \frac{t_W}{b_W}k_W; \quad R_6^{-1} = k_f; \quad R_{eq}^{-1} = k_{r,\mathrm{eff}} \tag{22}$$

Combining Eqs. (15), (18), (21) and (22) with subsequent manipulation gives:

$$k_{r,\mathrm{eff}} = \left[(1 - \sqrt{\phi+\xi}) + \frac{\sqrt{\phi+\xi} - \sqrt{\phi}}{(1 - \sqrt{\phi+\xi}) + (k_W/k_S)\sqrt{\phi+\xi}} + \frac{\sqrt{\phi}}{(1 - \sqrt{\phi+\xi}) + (k_W/k_S)(\sqrt{\phi+\xi} - \sqrt{\phi}) + (k_f/k_S)\sqrt{\phi+\xi}}\right]^{-1} k_S \tag{23}$$

This equation is the same as quoted in [4]. In the absence of washcoat, the expression reduces to:

$$k_{r,\mathrm{eff}} = \left[1 - \sqrt{\phi} + \frac{\sqrt{\phi}}{1 - \sqrt{\phi} + (k_f/k_S)\sqrt{\phi}}\right]^{-1} k_S \tag{24}$$

Eq. (24) was given in [3]. For reference purposes, we will refer to this model as the series model. All of the equations have the general form:

$$k_{r,\mathrm{eff}} = G\, k_S \tag{25}$$

The effective transverse conductivity is thus a function of the substrate conductivity and the G factor, which depends on the physical properties, i.e.:

$$G = f\left(\phi, \xi, \frac{k_W}{k_S}, \frac{k_f}{k_S}\right) \tag{26}$$

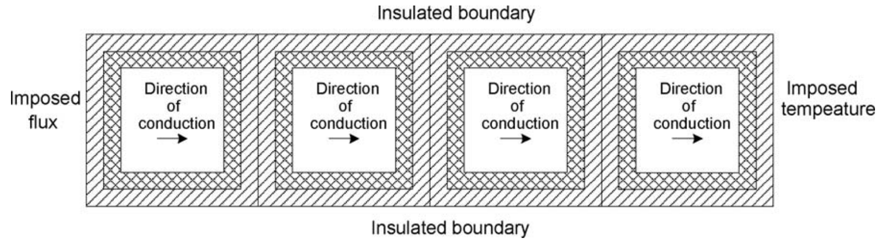

Fig. 3. A single row of four cells with washcoat showing location of imposed boundary conditions.

One of the advantages of these theoretical models is that they satisfy the limiting conditions. For example, consider the cases for the monoliths without washcoat, Eqs. (20) and (24). If the porosity is set to zero, corresponding to solid substrate, then G has a value of 1 and $k_{r,\mathrm{eff}} = k_S$. If the porosity is unity, then $G = k_f/k_S$ and $k_{r,\mathrm{eff}} = k_f$. Furthermore, if the solid and fluid thermal conductivities are the same, the model also gives the correct effective value.

3. Numerical model for the effective thermal conductivity

As noted in the preceding section, the electrical analogy for parallel thermal resistances is not exact, because it assumes one dimensional heat transfer, which is not the case. Typically the real value lies between that predicted by the parallel and series models. A more accurate value for the effective thermal conductivity can be determined using a numerical solution for the underlying energy balance equation in two dimensions. The solution is relatively straight forward using, for example, finite element methods. In this work we used the software package COMSOL Multiphysics Version 3.5a. The methodology employed was as follows.

A single row of cells was initially selected. Each sub-domain, which consisted of either fluid, substrate or washcoat, was discretized with a finite element mesh of P2 triangles. The geometry for four cells with the boundary conditions labelled is shown in Fig. 3. As shown, the top and bottom of the row are insulated (zero flux condition). A constant temperature was imposed on one side, and a constant heat flux on the other. The solution was then effected and the average temperature along the latter side computed by integration. The effective thermal conductivity was then computed from the formula:

$$q'' = k_{r,\mathrm{eff}} \frac{\Delta T}{W} \tag{27}$$

The temperature difference is based on the imposed and the computed average temperatures. Preliminary investigation showed that there was a small change in the computed value of effective thermal conductivity when fewer than four cells were used. As an alternative, both sides were given an imposed temperature and the resulting flux computed by integration along one face. The two results were the same for all cases, provided that there was at least four cells.

4. Results and discussion

There are many variations of properties that might be of interest, either practically or academically. A large number of simulations were performed in both bare and washcoated monoliths to examine the effects of the various parameters. These include: thermal conductivity of both substrate and washcoat, fraction of substrate and washcoat in monolith, shape of the washcoat and shape of the monolith cells. In the following sub-sections a selection of these results is shown, which illustrate the main findings of the investigation. The results are presented in terms of the G factor introduced in Eq. (25). All of the results use a fluid thermal conductivity of 0.06 W/(m K). This stricture does not limit the generality of the results, because, as seen earlier, the significant parameter is the ratio of fluid and solid thermal conductivities.

4.1. Blank substrate–model comparison

In this section we compare the performance of the two limiting theoretical models to the more accurate numerical solution for the case of both the coated and bare monolith. We begin with the most typical structure for ceramic monoliths; a square cell with a 75% porosity. In the first instance we consider the case without washcoat. Fig. 4 shows how the G factor changes with the solid thermal conductivity. The values predicted by the series and parallel models are also given. The G factor has asymptotic limits at both extremes of k_S. As the solid thermal conductivity approaches

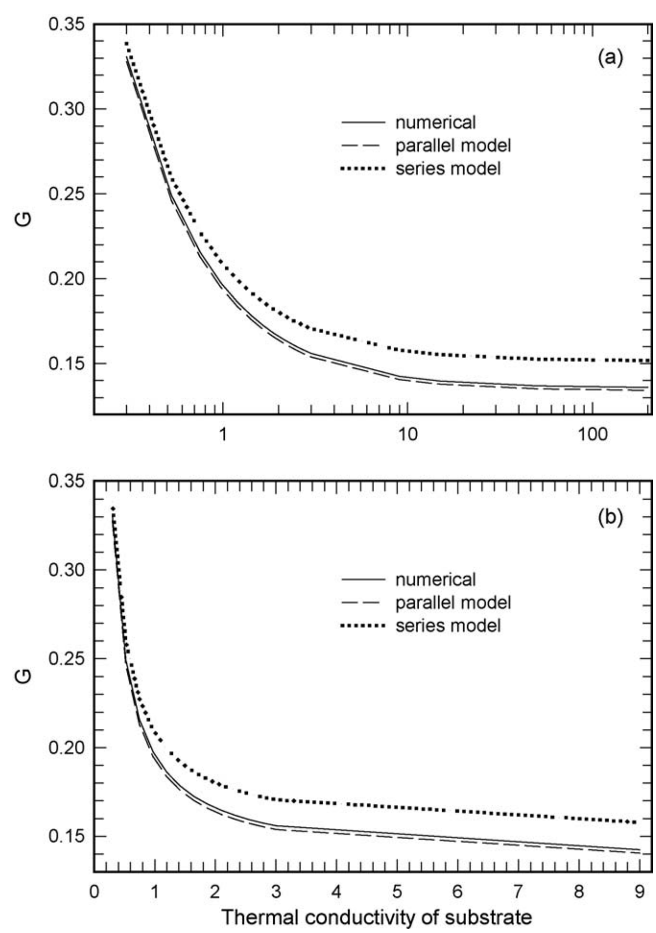

Fig. 4. Variation of the G factor with solid thermal conductivity for a blank monolith of porosity of 75%. (a) Full range on a log scale, (b) range at low conductivity only.

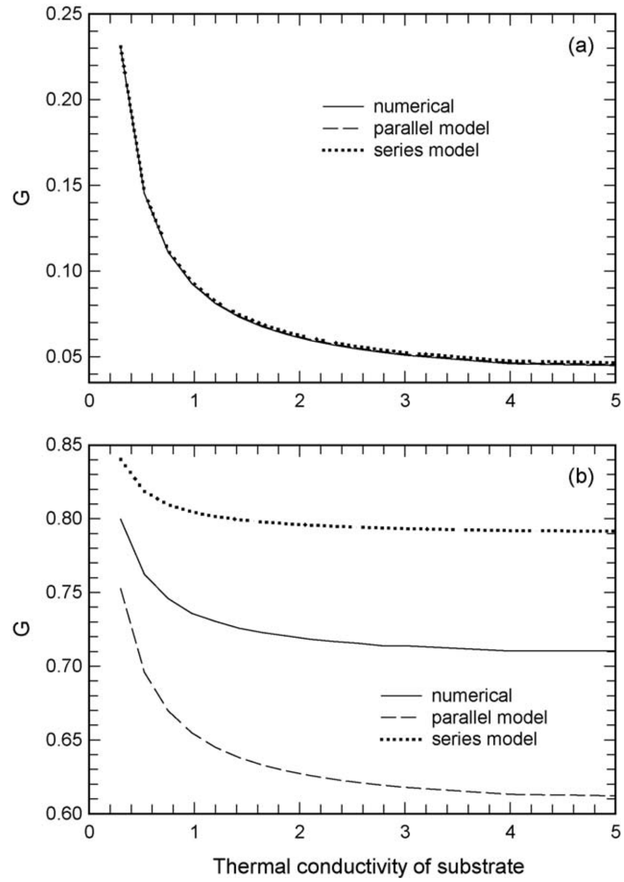

Fig. 5. Variation of the *G* factor with solid thermal conductivity for a blank monolith of porosity of (a) 93% and, (b) 16%.

that of the fluid, *G* approaches unity. As k_S increases, *G* approaches a limit of 0.134, and does not change much after a k_S value of about 10. The parallel model gives a much better prediction for the effective thermal conductivity than the series model.

For a blank monolith, the other factor of interest is the effect of porosity on the effective thermal conductivity. Fig. 5 shows the extremes of (a) high (94%) and (b) low (16%) porosity. Very high porosity can result when metal substrates are used, although low porosity is likely of little practical interest. The main conclusions are that high porosity gives a low *G* value, and that the series and parallel models are in close agreement. At low porosity, the *G* factor increases, the gap between the predictions of the series and parallel models widens, and the numerical solutions move closer to the serial model. Fig. 6 shows a summary of the porosity effects at a constant thermal conductivity of 1.2 W/(m K). It is worthwhile comparing a typical Cordierite monolith (thermal conductivity 1.5 W/(m K)) of 75% porosity with that of a steel monolith (thermal conductivity 15 W/(m K))with 93% porosity. The effective thermal conductivity of the former would be about 0.25 W/(m K) and the latter about 0.75 W/(m K).

4.2. Effect of washcoat

In this section the effect of adding some washcoat to the monolith is studied. Generally speaking the shape of the washcoat is irregular, with fillets tending to form in the corners of the channel. In the first instance, however, we show the result for a uniformly distributed washcoat. We consider the case of a base monolith with 75% porosity and add 10% by volume of washcoat. Because of the nature of the catalytic washcoat, we consider only a

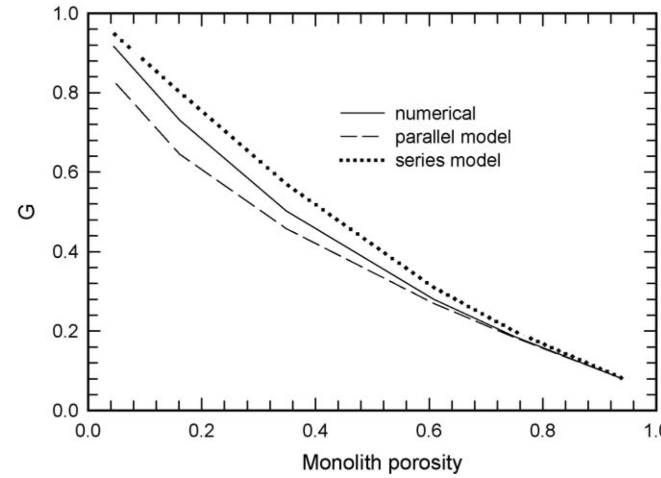

Fig. 6. Variation of the *G* factor with porosity for an uncoated monolith.

limited range of thermal conductivities, typical of washcoat materials. Fig. 7(a) shows the variation of *G* with washcoat thermal conductivity of 0.75 W/(m K), as well as the model predictions, while Fig. 7(b) shows the effect of changing the thermal conductivity of the washcoat over a small range, and includes the case for no washcoat.

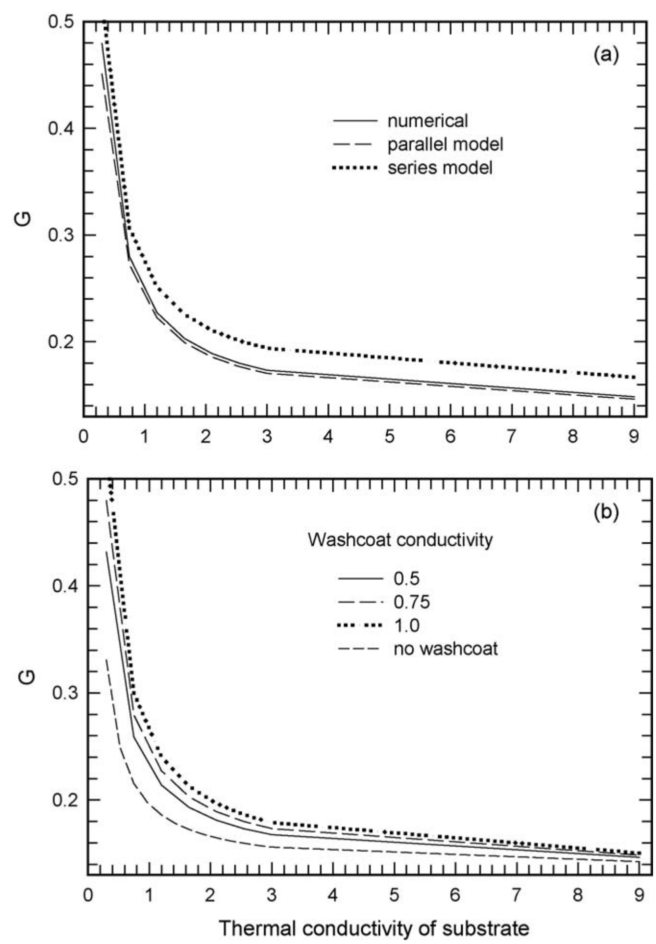

Fig. 7. (a) Variation of *G* with monolith thermal conductivity at a washcoat conductivity of 0.75 W/(m K), as well as the model predictions. (b) Effect of changing the thermal conductivity of the washcoat over a small range, and includes the case for no washcoat.

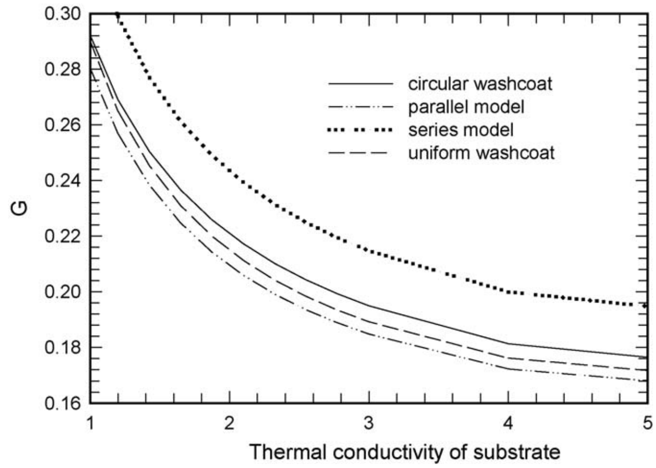

Fig. 8. Effect of washcoat shape on the *G* value, with comparison to the network models.

For this geometry, the parallel model gives the better prediction, as was the case for the blank monolith. Adding washcoat increases the value of *G*, which is consistent with the previous results. Adding washcoat is equivalent to reducing the porosity, which increases *G* provided that the fluid has a lower thermal conductivity than the washcoat. Higher washcoat conductivity also gives higher *G*, which is expected. Generally the effect of adding washcoat is what is expected.

Fig. 8 shows the effect of the washcoat shape inside the channel. As noted earlier, the method of manufacture tends to leave fillets in the corners. In this illustration, we take the extreme case where the inside surface of the washcoat is described by a circle. We compare it to the case having an equivalent amount of washcoat spread uniformly about the channel. (Note that the more realistic case is discussed in the following sections.) The porosity of the monolith substrate is 75%, while after the washcoat was applied the porosity is 56.8%. Note that the circular washcoat gives a *G* value about 3% higher.

4.3. Effect of orientation

In the preceding sections the basic behaviour of the three models was shown, and it is seen that the theoretical models bracket the real solution, as expected. However, there is a further complication in a real monolith, in that the conduction will occur at various directions through the cells. That is, conduction does not occur in the direction shown in Fig. 1. Therefore, to capture the orientation effect, conduction through a "web" of monolith was examined. We consider a quarter section of a circular monolith, to retain a 2D problem, as shown in Fig. 9. Constant temperature boundary conditions were imposed on the two circular boundaries, and the effective thermal conductivity was back calculated from the observed heat flow rate.

Fig. 10 shows the difference in the value of *G* computed for a blank monolith using the web and the four cell domains for a porosity of 75% and 61%. It is seen that for the 75% case there is essentially no difference between the solutions, while for the 61% case the web solution gives a *G* value about 4% higher than the row of cells model.

4.4. Effect of cell shape

For the next set of results the monolith web domains were used to study the effect of the structure on the effective thermal conductivity. Three classical cell shapes were selected: square, triangle and hexagonal. The uncoated monolith porosity in each case was 75%. For each shape, two washcoat shapes were used, with a washcoat loading of 10% by volume. In one loading, the washcoat was uniform and in the other the washcoat had fillets in the corners. The uncoated web geometry for the square cells is shown in Fig. 9; for hexagons and triangles it was similar. The cell shapes with and without washcoat are shown in Fig. 11. With the corner fillet case, the washcoat thickness on the sides is 10 μm. The results are presented in Fig. 12. The following observations can be made. For the uncoated monolith, the triangles and squares have very close effective thermal conductivities. The lowest effective thermal conductivity was observed for the hexagons. In all cases, adding washcoat increases the value of *G*, with the fillet shape giving the largest increase. The effect of washcoat shape is the least pronounced for the hexagonal case, likely because, even with fillets, the washcoat is more uniform. The effect of washcoat shape is largest for the triangular case. Overall, the highest effective thermal conductivity is achieved using triangular cells with a non-uniform washcoat.

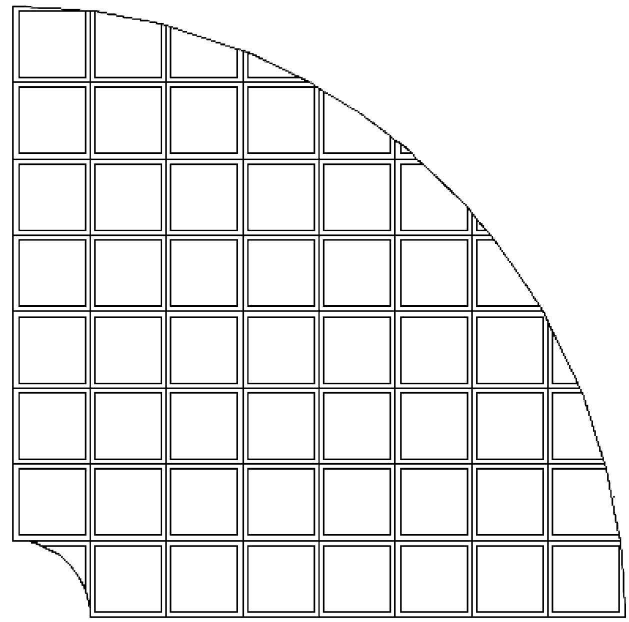

Fig. 9. Solution domain for the full monolith simulation (web of cells). A quarter circular section is used to take advantage of symmetry.

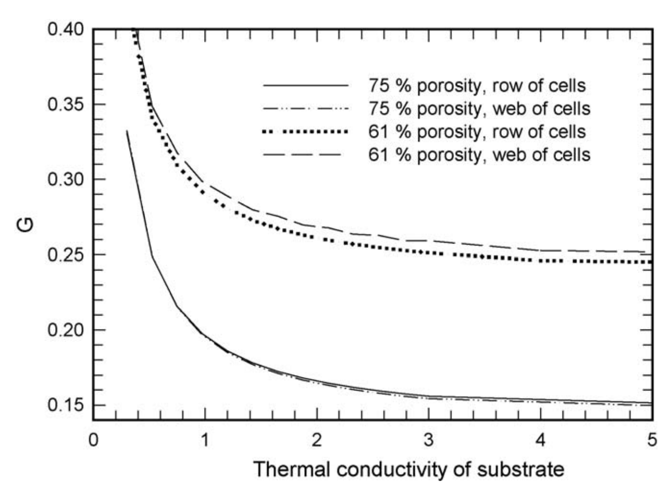

Fig. 10. Comparison of the *G* value for a row of four cells to that obtained on a web of cells for monolith porosities of 75% and 61%.

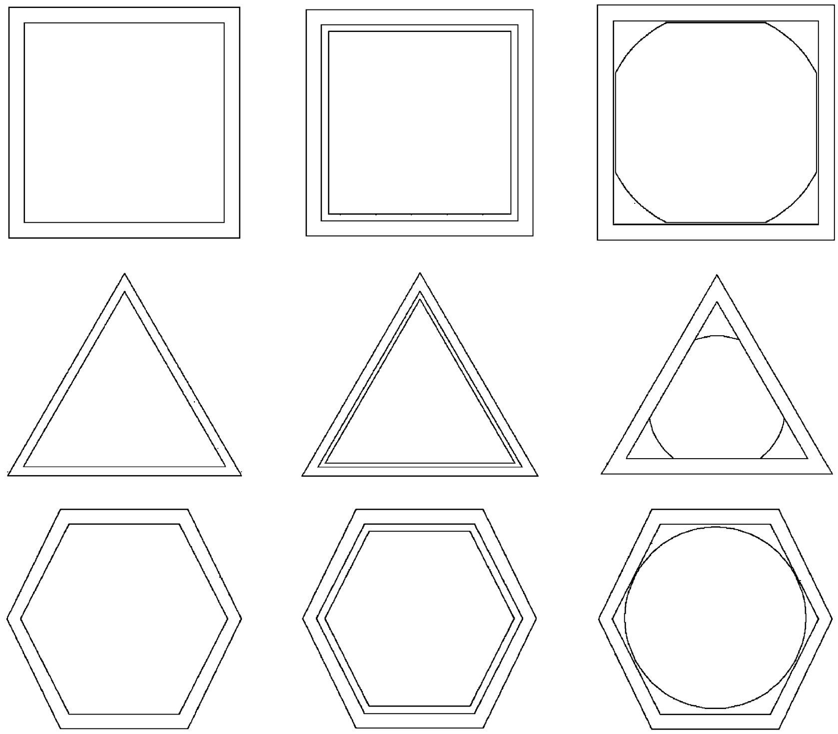

Fig. 11. Summary of the nine monolith geometries used for the tests in the web.

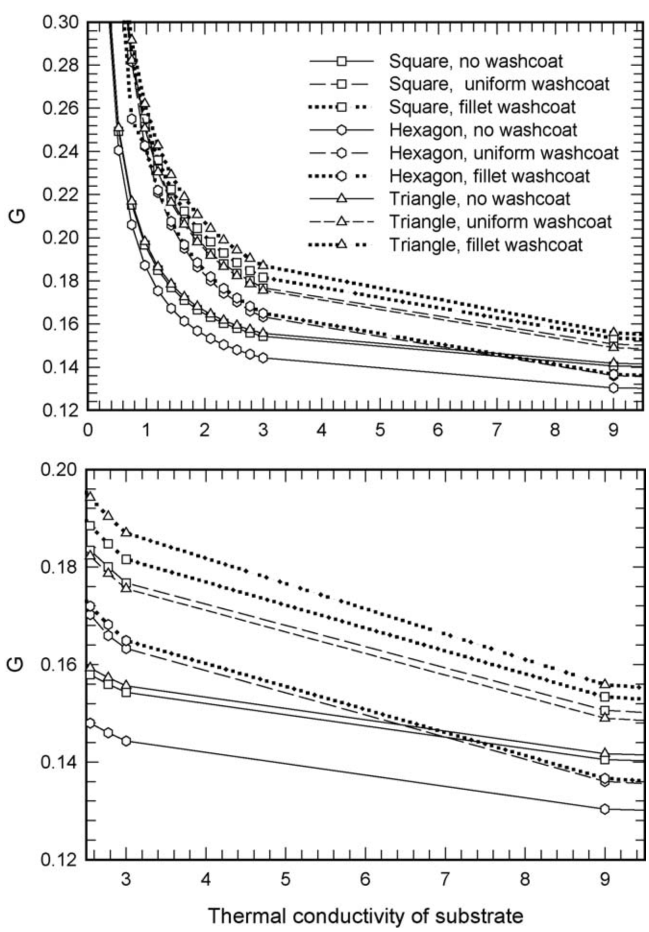

Fig. 12. Variation of the value of G with substrate type and washcoat geometry. The substrate occupies 25% by volume and the washcoat 10% (if present). The top graph shows the full scale and the bottom a limited range for clarity.

5. Conclusions

This investigation has examined the effective transverse effective thermal conductivity in monolith systems. The following are the main conclusions.

- A numerical model of the real structure is relatively simple to build and not time consuming to run using readily available commercial computer software.
- The most accurate results for effective thermal conductivity are obtained using a model of the real monolith structure accounting for all heat flow directions.
- A small scale numerical model consisting of a row of cells is a reasonable approximation.
- Models based on the electrical network analogy of resistances in series and parallel can be used to provide limits for the solution. For high porosity monoliths a network model based on parallel resistances provides the best answer.
- Application of a washcoat and its geometry affects the effective thermal conductivity.
- Above a critical value of monolith substrate thermal conductivity, the effective thermal conductivity varies directly with the substrate conductivity.
- Monoliths with square and triangular channels have similar effective thermal conductivity, and hexagon shaped cells are significantly lower, everything else being equal.

References

[1] R.E. Hayes, S.T. Kolaczkowski, Introduction to Catalytic Combustion, Gordon and Breach, London, 1997.
[2] F.P. Incropera, D.P. DeWitt, T.L. Bergman, A.S. Lavine, Introduction to Heat Transfer, 5th edition, Wiley, New York, 2007.
[3] G. Groppi, E. Tronconi, AIChE Journal 42 (8) (1996) 2382.
[4] G. Groppi, E. Tronconi, Chemical Engineering Science 55 (2000) 2161.
[5] A.G. Konstandopoulos, M. Kostoolou, N. Vlachos, E. Kladopoulou, in: G.B. Marin (Ed.), Advances in Chemical Engineering, vol. 33, Elsevier, Amsterdam, 2008 , p. 254 (Chapter 4).
[6] F. Zhang, R.E. Hayes, S.T. Kolaczkowski, Chemical Engineering Research and Design 82 (A4) (2004) 481.